Image potential matched self-consistently to an effective potential for simple-metal surfaces

Adam Kiejna
Institute of Experimental Physics, University of Wrocław, ul. Cybulskiego 36, 50-205 Wrocław, Poland

(Received 20 November 1990; revised manuscript received 28 February 1991)

Using density-functional theory, the one-electron effective potential is matched self-consistently to the image-potential shape outside the surface of semi-infinite jellium and of real, simple metals. For real metals, the discrete-lattice effects are taken into account, following the variational method of Monnier and Perdew. The image-plane position of semi-infinite jellium, of Al(111), and of the (110) face of Li, Na, K, Rb, and Cs is determined. We find that for a given surface, the incorporation of the discrete lattice influences the location of the image plane much more strongly than the nonlocal effects.

The application of density-functional formalism[1] has contributed to much progress in the study of the electronic structure of metallic surfaces.[2] Lang and Kohn[3,4] (LK) solved the Kohn-Sham equations[1] for the jellium surface using the local density approximation (LDA) for the exchange and correlation effects, and obtained the electron-density profiles and the one-electron effective potentials. They calculated also, within first-order perturbation theory, the effect of the discrete-lattice potentials on the surface energy and work function and image-plane position.[5] Although the LDA did not give the image-potential behavior, $-1/4x$, of the effective potential far outside the metal surface, it had very little influence on the calculated work functions and surface energies. This was due to the fact that the image-potential effect is important in a region where the electron density is very small compared with the average value in the bulk metal.

The LK work was generalized later by Monnier and Perdew[6] (MP), who included the ionic lattice potential in a variational, self-consistent way. Their calculation brought considerable differences in calculated electron-density profiles at a given crystal face compared with the jellium profiles. It led also to improved calculated surface energies[6] and work functions.[7] Another calculational scheme was presented more recently by Serena, Soler, and Garcia (hereafter referred to as SSG-I), who solved the Kohn-Sham equations for a finite metallic slab,[8] including the local ionic pseudopotentials. Their results for the work function were in rough agreement with those obtained in the variational self-consistent scheme.[7]

In recent years the question of the validity of the LDA has become more important for two reasons. Firstly, the variational method, which does not assume a slow spatial variation of the electron density, was developed and applied to metal surfaces,[9,10] yielding surface energies larger than LDA values. Secondly, a correct description of the asymptotic limit ($x \to \infty$) of effective potential has become crucial in the studies of the existence of image states at metal surfaces[11] and evaluation of the tunnel current across the surface barrier in scanning tunneling microscopy.[12]

A number of improvements to the LDA have been developed.[2] None of them, however, seems to be fully satisfactory. For example, the Langreth-Mehl[13] nonlocal correction leads to an increase in surface energies but does not give the correct behavior of the potential far away from the surface.[14] Some other calculations[15,16] which reproduce the image potential at large distances yield very controversial results for the position of the image plane. On the other hand, Serena, Soler, and Garcia (hereafter, SSG-II) have proposed[17] a simple computational scheme where the classical image-potential limit is matched self-consistently to the local exchange-correlation potential. This procedure leads to a small reduction in the value of the image-plane position relative to the LDA results.

In this Brief Report we apply the scheme of SSG-II to recalculate the image-plane position for the semi-infinite jellium in order to eliminate any finite-size effects which might affect the original calculation for the jellium slab.[17] The main purpose of this work is to extend the method of SSG-II to the case of real, simple metals and calculate the image-plane position at the most compact surface plane of Al and alkali metals.

Our self-consistent procedure follows the MP scheme.[6] The electron density $n(\mathbf{r})$ is constructed from the one-electron wave functions which satisfy the Schrödinger equation with the effective potential $v_{\text{eff}}[n(\mathbf{r})]$ being the sum of electrostatic and exchange-correlation contributions. The electrostatic potential[18] in turn can be written as $\phi[n(\mathbf{r})]+\delta v(\mathbf{r})$ where $[\phi[n(\mathbf{r})]$ is the sum of the potential from the ions and the Coulomb potential from the other electrons, and $\delta v(\mathbf{r})$ is the difference between the potential of the discrete lattice and the potential of the neutralizing positive background $n_+(\mathbf{r})$. For a semi-infinite metal filling the half-space $x<0$, $n_+(\mathbf{r})=\bar{n}\Theta(-x)$ where $\bar{n}=3/4\pi r_s^3$ is the average electron density in the bulk and $\Theta(x)$ is the unit-step function. In the method of MP the lattice term $\delta v(\mathbf{r})$ is replaced by a simple parametrized function of the form $C\Theta(-x)$, where the optimum value of $C=C_m$ was determined from the minimum of surface energy. In this way

TABLE I. Positions x_0 (in bohrs) of the image plane obtained in this work for the jellium densities, compared with the LDA (Refs. 5 and 17) and nonlocal results from Serena, Soler, and Garcia (SSG-II, Ref. 17) and Ossicini, Finocchi, and Bertoni (OFB, Ref. 22).

	LDA				
r_s	Ref. 5	Ref. 17	This work	SSG-II	OFB
2	1.6	1.57	1.56	1.49	1.48
3		1.35	1.37	1.24	1.28
4	1.3	1.25	1.28	1.13	1.23
5		1.17	1.23	1.08	
6	1.2	1.10	1.19	1.02	

the self-consistent solution of the three-dimensional Schrödinger equation can be reduced to the solution of a one-dimensional problem.

Following the idea of SSG-II, the local exchange-correlation potential $v_{xc}^{L}[n]$ in the metal,

$$v_{xc}^{L}[n]=d\{n\varepsilon_{xc}[n]\}/dn \ , \tag{1}$$

where $\varepsilon_{xc}[n]$ is the sum of exchange and correlation[19] energy per particle in an electron gas of density n, is matched at the image-plane position x_0 to the nonlocal potential of the form

$$v_{xc}^{NL}(x)=-\frac{1-[1+b(x-x_0)/4]e^{-b(x-x_0)}}{4(x-x_0)} \ . \tag{2}$$

The latter expression results from the integration of the spherical potential[17] produced by the local exchange-correlation hole. The parameter b is determined from the requirement of continuity of v_{xc} at x_0 to give $b=-\frac{16}{3}v_{xc}^{L}(x_0)$. The value of x_0 is calculated self-consistently by solving at every iteration the Schrödinger equation for a neutral surface and for a surface with a small surface excess charge Σ. The center of mass $\bar{x}$ of the induced surface charge was calculated after each iteration from the expression

$$\bar{x}=\int_{-\infty}^{\infty} x\,\delta n(x)dx \Big/ \int_{-\infty}^{\infty}\delta n(x)dx \ , \tag{3}$$

where $\delta n(x)=n(x)-n_{\Sigma}(x)$ is the difference between the electron-density profiles for a neutral and charged surface, and used as x_0 to calculate the potential for the next iteration. In this way the effective potential is matched self-consistently to its image-potential-like form at large distances.

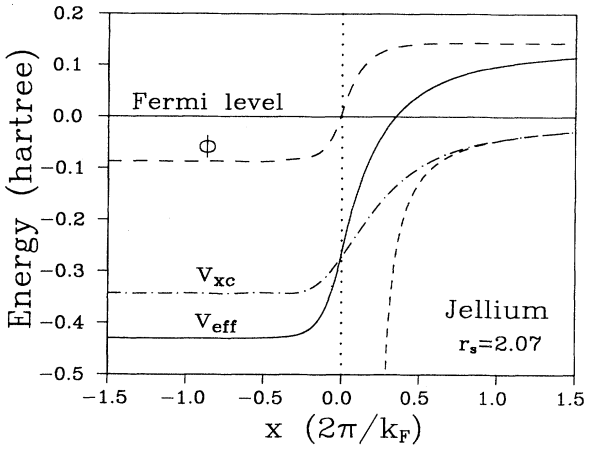

FIG. 1. The effective one-electron potential v_{eff} with electrostatic (ϕ) and exchange-correlation (v_{xc}) part for a jellium surface with $r_s=2.07$. The classical image potential is also shown for comparison (dashed curve).

The convergence of this self-consistent procedure was controlled through such criteria as (i) the charge neutrality condition, (ii) the agreement between computed surface dipole barrier $\phi(\infty)-\phi(-\infty)$ and the surface dipole moment, and (iii) the Budd-Vannimenus theorem[20,6] relating the surface electrostatic potential to bulk properties.

For the jellium surface the calculated exchange-correlation potential (Fig. 1) matches continuously the classical image-potential form. The corresponding electron-density profile is very similar to the LDA profile calculated by LK. A consequence of this fact is the insensitivity of the surface energies and work functions to the use of the nonlocal potential. In the whole range of metallic bulk electron densities considered, $2\le r_s\le 6$, the surface energy varies by not more than 2.5% and the work function is within 0.02 eV with respect to the LDA value. The results for the image-plane position computed self-consistently from Eq. (3) which are listed in Table I

TABLE II. The work function (in eV) for the most densely packed plane of simple metals, obtained in this work for the image-potential limit matched to the LDA. The LDA results from Serena, Soler, and Garcia (SSG-I, Ref. 8) and nonlocal ones from Finocchi, Bertoni, and Ossicini (FBO, Ref. 23), and Zhang, Langreth, and Perdew (ZLP, Ref. 14) are also shown.

r_s	Metal	Face	Present work	SSG-I	FBO	ZLP	Experiment[a]
2.07	Al	(111)	4.18	4.18	4.18	4.26	4.19
3.28	Li	(110)	3.61	3.63		3.75	3.1
3.99	Na	(110)	3.11	3.11	2.94	3.39	2.7
4.96	K	(110)	2.74			3.09	2.39
5.23	Rb	(110)	2.56			2.88	2.21
5.63	Cs	(110)	2.44	2.62		2.78	2.12

[a]Reference 9.

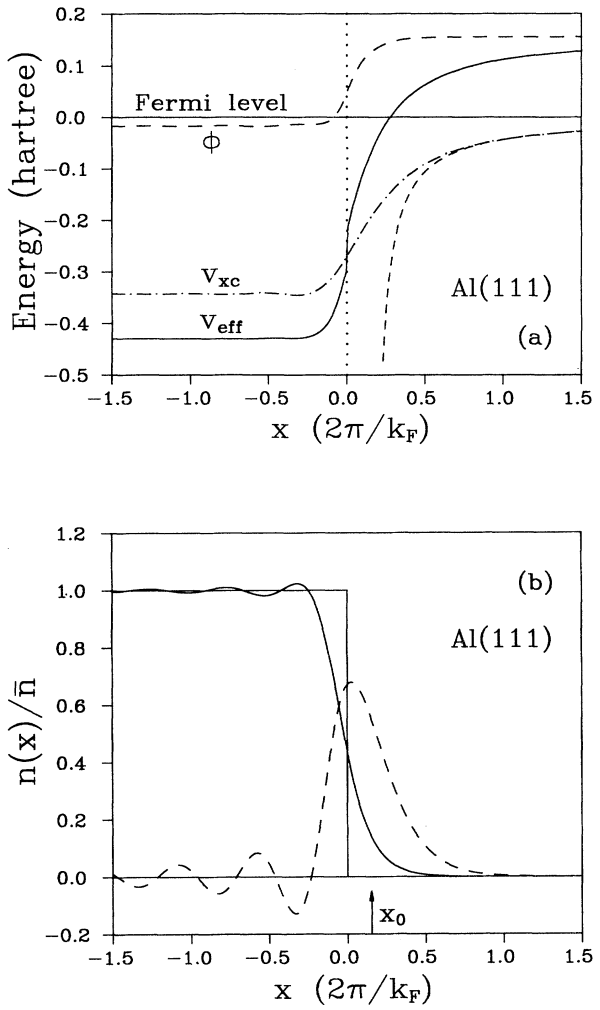

FIG. 2. (a) The effective potential and its components for the real, metal Al(111) face ($C_m = -1.9$ eV). The effect of the step function $C_m\Theta(-x)$ on the v_{eff} curve is visible. The lower part (b) shows the plot of corresponding electron-density profile (solid line) and the induced surface charge density $\delta n(x)$ times 100 (dashed curve). The arrow indicates the position of the image plane.

show very good agreement with the values determined originally by LK (Ref. 5) in the LDA.[21] Note that for $r_s \geq 3$ these are slightly higher than the numbers reported by SSG-II for the LDA. For the higher bulk electron densities the positions determined in this paper are closer to the nonlocal results of Ossicini, Finocchi, and Bertoni[22] for the semi-infinite jellium than to the nonlocal ones calculated by SSG-II. The difference between our results and those of SSG-II may stem from the difference in geometry of the system considered. Another explanation of this discrepancy may be that the positions x_0 given by SSG-II and determined for the small excess charge were not extrapolated to the zero-charge limit as has been done in the present work.

In Fig. 2 we have displayed the nonlocal effective potential and the corresponding electron-density profile for

TABLE III. The image-plane position (in bohrs) for the real, metal planes obtained for the nonlocal potential of this work. x_0 is the position relative to the jellium edge while x_{im} is determined relative to the location of the first lattice plane in a metal [see Eq. (4)]. The local values from Serena, Soler, and Garcia (SSG-I, Ref. 8) are also given.

			x_{im}	
Metal	Face	x_0	This work	SSG-I
Al	(111)	1.12	3.32	3.3
Li	(110)	0.83	3.18	3.2
Na	(110)	1.49	4.35	
K	(110)	1.64	5.20	
Rb	(110)	2.60	6.35	
Cs	(110)	3.13	7.17	

the Al(111) face. Since the matching of the LDA potential to the image-potential shape outside the metal affects the effective potential at relatively large distances from the surface, its effect on the surface energy is small. Therefore, in this work we did not minimize the surface energy with respect to the parameter C and the local values of $C = C_m$ determined[6] by MP were used. Actually, the calculated surface energies at the most densely packed plane of all metals considered are equal to the LDA values given in Ref. 6. The work functions—similarly, as for the jellium surface—differ by ~ 0.02 eV from the local values. We have found also very good agreement of our nonlocal work functions calculated from the "change in self-consistent-field" expression[7] (Table II) with the local ones obtained in the slab model.[8] The value of the work function of Al(111) agrees also with that calculated beyond the LDA.[23] The relatively large difference between the values computed by us and those of Zhang, Langreth, and Perdew[14] is due mainly to the different correlation energy functional used.

Let us consider now the effect of the crystal lattice structure on the image-plane position. For a jellium surface the image-plane position x_0 was determined from Eq. (3) as the position of the centroid of induced excess charge relative to the background edge. Then the effective surface in a metal is located at

$$x_{\text{im}} = x_0 + d/2 \tag{4}$$

in front of the first atomic layer, where d is the interplanar spacing. If one employs in Eq. (4) the x_0 value for the jellium, it leads to a strong dependence of x_{im} on the crystallographic orientation.[8] This strong dependence, however, is greatly reduced when x_0 is determined not from a jellium calculation but from the one performed for a real metal in the variational self-consistent scheme. The resulting[24] sequence of x_{im} agrees with the sequence obtained by SSG-I. It is completely reversed, however, compared with the one resulting from the jellium model which gives the face-independent x_0 contribution. Therefore, in a realistic calculation of x_{im}, one should use the x_0 values determined for a given metal face. The calculated change $\delta n(x)$ in the electron-density distribution

induced by an electric field perpendicular to the Al(111) face is displayed in Fig. 2. The curve was obtained for a total surface excess charge $\Sigma=5\times10^{-4}$. In Table III we give the results for the image-plane position at the most densely packed planes of Al and alkali metals compared with the local results of SSG-I for the finite slab model. Inspecting the numbers listed for x_0 in Table III and the corresponding ones for jellium (Table I), it can be seen that the discrete-lattice effects are much stronger on the centroid of the excess charge than nonlocal effects. The incorporation of lattice structure leads to substantial changes in the position x_0 of the centroid. This is particularly visible for Li, Rb, and Cs for which the value of variational parameter C_m representing lattice effects is of the order of magnitude of the Fermi energy.[6]

In conclusion the self-consistent matching procedure of the LDA potential to the image-potential limit was extended to real, metal surfaces. The positions of the image plane calculated for the semi-infinite jellium and real, metal surfaces remain practically unaffected by the matching procedure and agree well with those determined in the LDA.

The author thanks Professor J. P. Perdew for providing the Monnier-Perdew computer code for metal-surface calculations. This work was supported by a grant from the Ministry of National Education (Poland).

[1]P. Hohenberg and W. Kohn, Phys. Rev. **136**, B664 (1964); W. Kohn and L. J. Sham, *ibid.* **140**, A1133 (1965).
[2]N. D. Lang, in *Theory of the Inhomogeneous Electron Gas,* edited by S. Lundqvist and N. H. March (Plenum, New York, 1983).
[3]N. D. Lang and W. Kohn, Phys. Rev. B **1**, 4555 (1970).
[4]N. D. Land and W. Kohn, Phys. Rev. B **3**, 1215 (1971).
[5]N. D. Lang and W. Kohn, Phys. Rev. B **7**, 3541 (1973).
[6]R. Monnier and J. P. Perdew, Phys. Rev. B **17**, 2595 (1978); **22**, 1124(E) (1980).
[7]R. Monnier, J. P. Perdew, D. C. Langreth, and J. W. Wilkins, Phys. Rev. B **18**, 656 (1978).
[8]P. A. Serena, J. M. Soler, and N. Garcia, Phys. Rev. B **37**, 8701 (1988).
[9]X. Sun, M. Farjam, and C.-W. Woo, Phys. Rev. B **28**, 5599 (1983).
[10]E. Krotscheck, W. Kohn, and G.-X. Qian, Phys. Rev. B **32**, 5693 (1985).
[11]N. V. Smith and D. P. Woodruff, Prog. Surf. Sci. **21**, 295 (1986).
[12]G. Binnig, H. Rohrer, C. Gerber, and E. Weibel, Phys. Rev. Lett. **50**, 120 (1983).
[13]D. C. Langreth and M. J. Mehl, Phys. Rev. Lett. **47**, 446 (1981); Phys. Rev. B **28**, 1809 (1983).
[14]Z. Y. Zhang, D. C. Langreth, and J. P. Perdew, Phys. Rev. B **41**, 5674 (1990).
[15]S. Ossicini, C. M. Bertoni, and P. Gies, Surf. Sci. **178**, 244 (1986).
[16]A. G. Eguiluz and W. Hanke, Phys. Rev. B **39**, 10 433 (1989).
[17]P. A. Serena, J. M. Soler, and N. Garcia, Phys. Rev. B **34**, 6767 (1986).
[18]Hartree atomic units are used unless stated otherwise.
[19]To maintain contact with previous calculations the Wigner interpolation formula for the correlation energy $\varepsilon_c=-0.44/(r_s+7.8)$ was employed in this work.
[20]H. F. Budd and J. Vannimenus, Phys. Rev. Lett. **31**, 1218 (1973); **31**, 1430(E) (1973).
[21]As we have checked the use of the correlation energy of D. M. Ceperley and B. J. Alder [Phys. Rev. Lett. **45**, 566 (1980)] parametrized by J. P. Perdew and A. Zunger [Phys. Rev. B **23**, 5048 (1981)] leads only to a very small ($\lesssim0.02$ a.u.) shift of x_0 towards the surface of jellium ($r_s=2,3,\ldots,6$) and the real Al(111).
[22]S. Ossicini, F. Finocchi, and C. M. Bertoni, Surf. Sci. **189/190**, 776 (1987).
[23]F. Finocchi, C. M. Bertoni, and S. Ossicini, Vacuum **41**, 535 (1990).
[24]Using the numbers given in the caption to Fig. 1 in Ref. 7, one gets the following for the $x_{\rm im}$: 3.30, 3.74, and 3.92 a.u. at (111), (100), and (110) faces of Al.